Jurnal JEETech: Vol. 6 No. 2 Tahun 2025
Journal Of Electrical Engineering And Technology
https://ejournal.ft-undar.ac.id/index.php/jeetech
DOI: https://doi.org/10.32492/jeetech.v6i2.6207
e-ISSN: 2722-5321
p-ISSN: 2964-7320

Performance Analysis of Building-Embedded Loop Antenna Systems for Smart City IoT Networks

[1]Farhan Rezki Arifin, [2*]Nurmayanti Zain, [3]Lompo Ramos Emakarim
[1,2,3]Department of Electrical Engineering, University of Cokroaminoto Makassar, Tamalanrea-Makassar, Indonesia
[1]farhan403@ucm-si.ac.id, [2]nurmayanti.zain@ucm-si.ac.id, [3]lompo_ramos@ucm-si.ac.id

Article Info

Article history:

Received: 28 October 2025
Revised: 11 November 2025
Accepted: 20 November 2025

Keyword:

Building-Integrated System;
Embedded Antenna;
IoT Networks;
Performance Analysis;
Smart City

ABSTRACT

The increasing demand for seamless connectivity in Smart City environments has encouraged the integration of communication systems directly within building infrastructures. This study presents the performance analysis of a building-embedded loop antenna system designed for sub-GHz Internet of Things (IoT) applications. The proposed antenna, made of stainless steel and embedded in a reinforced concrete column, was modeled and simulated using Ansys HFSS (High Frequency Structure Simulator) based on the Finite Element Method (FEM). Analytical and full-wave simulations were conducted to evaluate key electromagnetic parameters, including return loss, voltage standing wave ratio (VSWR), impedance bandwidth, and radiation characteristics. The results showed that the antenna achieved resonance at 700 MHz with a return loss of –20.95 dB and a VSWR of 1.196, demonstrating excellent impedance matching. The impedance bandwidth covered 563–939 MHz, ensuring compatibility with various IoT protocols such as LoRaWAN, NB-IoT, Z-Wave, and ZigBee. Despite reduced gain due to dielectric absorption and coupling within the concrete medium, the antenna maintained an omnidirectional radiation pattern, suitable for low-power IoT nodes. These findings indicate that building-embedded loop antennas can function as integrated communication elements while preserving architectural integrity.

[*]***Corresponding Author:***
Nurmayanti Zain
Department of Electrical Engineering, University of Cokroaminoto Makassar, Tamalanrea-Makassar, Indonesia
Email: nurmayanti.zain@ucm-si.ac.id

Abstrak—Meningkatnya kebutuhan akan konektivitas tanpa hambatan di lingkungan *Smart City* mendorong integrasi sistem komunikasi langsung ke dalam infrastruktur bangunan. Penelitian ini menganalisis kinerja sistem antena loop tertanam pada kolom beton bertulang untuk aplikasi *Internet of Things (IoT)* pada sub-GHz. Antena berbahan baja nirkarat ini dimodelkan dan disimulasikan menggunakan Ansys HFSS *(High Frequency Structure Simulator)* berbasis *Finite Element Method (FEM)*. Analisis analitik dan simulasi *full-wave* dilakukan untuk mengevaluasi parameter elektromagnetik utama seperti *return loss*, *voltage standing wave ratio (VSWR)*, lebar pita impedansi, dan karakteristik radiasi. Hasil menunjukkan bahwa antena mencapai resonansi pada 700 MHz dengan *return loss* –20,95 dB dan VSWR 1,196, menandakan pencocokan impedansi yang baik. Lebar pita 563–939 MHz menunjukkan kompatibilitas dengan berbagai protokol IoT seperti LoRaWAN, NB-IoT, Z-Wave, dan ZigBee. Meskipun terjadi penurunan gain akibat penyerapan dielektrik dalam beton, antena tetap mempertahankan pola radiasi omnidireksional yang sesuai untuk node IoT berdaya rendah.

I. Introduction

The rapid global urbanization and the imperative for sustainable living have accelerated the development of smart city and smart buildings, transforming urban landscapes into interconnected, intelligent environments [1-3]. Integral to this transformation is the Internet of Things (IoT), which enables seamless communication among diverse physical devices to optimize smart city functions [4-6]. The effective integration of IoT technologies within building infrastructures is key to enhancing operational efficiency and adaptability [7], fostering responsive and intelligent urban systems. Furthermore, the emergence of smart materials is pivotal in reshaping engineering and infrastructure, offering innovative solutions for various design and functional challenges [8], [9]. The functionality of these complex networks is often underpinned by embedded systems, which provide the necessary control and processing capabilities for individual IoT devices and integrated communication modules [10].

A cornerstone of efficient IoT and smart building communication systems is the antenna, acting as the vital link between devices and the broader network [11], [12]. Contemporary antenna designs are increasingly driven by demands for compactness, optimal performance, and seamless integration into complex environments, including architectural structures [13-15]. A significant challenge arises when antennas are embedded within building materials such as concrete or wall composites, whose dielectric properties and conductive elements (e.g., galvanized steel [16]) can substantially influence electromagnetic wave propagation and antenna performance [17], [18]. Prior studies have investigated antenna embedding in dielectric media for 5G applications [19], explored electromagnetic-thermal interactions of wall-embedded antennas [20], and characterized transmission losses in such configurations [21]. Nevertheless, accurately predicting the performance of antennas embedded in heterogeneous building materials remains a complex task [22], often requiring sophisticated inspection methods [23]. The integration of embedded antennas into these structures is crucial for the overall functionality of embedded systems controlling the IoT network [24].

Among various antenna types, loop antennas offer distinct advantages such as relatively compact size and good radiation characteristics, making them suitable candidates for integration into confined spaces [11]. While general antenna embedding has been explored [25], the existing literature still presents a critical gap regarding the analytical performance of specific antenna geometries in severely constrained, conductive architectural environments.

The unique properties of loop antennas, coupled with the intricate electromagnetic environment within building materials, specifically the presence of metallic rebar structures, present distinct challenges and opportunities for optimizing signal propagation, especially for Low-Power Wide-Area Networks (LPWANs) like LoRaWAN (Long Range Wide Area Network) [26], NB-IoT (Narrowband Internet of Things), Z-wave, ZigBee, and emerging 5G technologies [27], [28]. Despite ongoing efforts to optimize embedded element patterns for antenna arrays [29] and based IEEE 802.11 MAC Protocol for Radar Networks [30], a comprehensive understanding of loop antenna performance when integrated into diverse rebar-containing building composites, forming a critical part of the overall embedded system for communication, is still evolving.

This study employs Ansys HFSS (High Frequency Structure Simulator), a three-dimensional electromagnetic solver based on the Finite Element Method (FEM), to obtain rigorous solutions of Maxwell's equations for high frequency structures. The work presents a conceptual and analytical investigation of stainless steel loop antennas embedded in concrete for Sub-GHz Smart City IoT applications, emphasizing key design parameters, resonance characteristics, and integration scenarios within representative urban environments. The research develops a systematic framework for evaluating and optimizing the electromagnetic performance of loop antennas when embedded in building materials, with particular attention to their role as integral components of communication infrastructures. The objectives include assessing the influence of material properties and embedding depths on antenna efficiency, radiation behavior, and impedance matching, while also identifying effective strategies for structural integration.

The novelty of this study lies in its comprehensive investigation of embedded loop antenna systems interacting with rebar structures, offering new insights into their electromagnetic behavior and demonstrating their applicability in Smart City IoT networks. The outcomes are expected to advance the development of unobtrusive, efficient, and reliable communication frameworks, thereby facilitating the realization of pervasive and intelligent urban environments.

II. Method

A. Simulation Methodology Flowchart

This study applies a simulation-based framework that integrates theoretical modeling, resonance analysis, and full-wave electromagnetic simulation to assess the potential of stainless steel structures embedded in buildings as loop antennas for sub-GHz Smart City communications. The investigation focuses on the 700 MHz band, a spectrum widely recognized for enabling long-range, low-power IoT connectivity [2], [5].

Simulation results are extracted from HFSS post-processing analysis, including S_{11} reflection coefficient, input impedance, and electric/magnetic field distributions. The data are analyzed to determine resonant frequency, bandwidth, and radiation patterns of the embedded loop antenna.

A flowchart illustrating the simulation methodology is presented in Figure 1, outlining the sequential process of analytical modeling, geometry construction, material assignment, simulation setup, and result analysis. This structured approach ensures that the study can be accurately reproduced in future research.

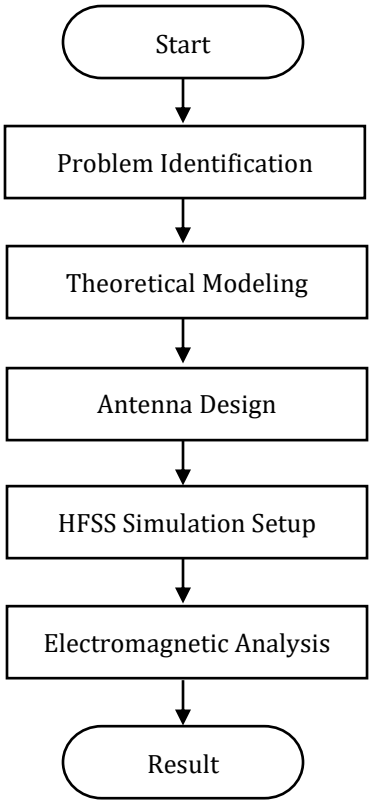

Figure 1. Simulation Methodology Flowchart

Flowchart illustrates the overall process of designing and simulating a building-embedded loop antenna. The study begins with identifying the problem and defining objectives for sub-GHz Smart City IoT communication. A theoretical model is developed to determine the target frequency and antenna dimensions. The antenna configuration is then designed and implemented in Ansys HFSS, where the structure, materials, and boundary conditions are defined. Electromagnetic analysis follows to evaluate reflection coefficients, field distributions, and coupling effects. Finally, simulation results are analyzed to identify resonant characteristics and assess the antenna's performance within the building structure.

B. Building-Embedded Loop Antenna Configuration

$L = \frac{1}{4}\lambda = \frac{c}{4f}$The resonant length of the loop antenna as a quarter-wavelength radiator is analytically determined based on Equation (1):

(1)

where:
c is the speed of light (3×10^8 m/s),
f is the target frequency (700 MHz).

With a resonant wavelength of 42.86 cm and assuming a 1:1 aspect ratio for the rectangular loop, both the loop length and width are determined to be 21.43 cm. When the finite diameter of the conductor is considered, the effective electrical dimensions are slightly reduced to approximately 21 cm × 21 cm, consistent with established diameter correction factors commonly applied in antenna optimization. The feed gap is set to 5 cm, and the feed section extends 6 cm from the edge of the gap to facilitate signal excitation and impedance matching.

This configuration as shown in Figure 2 enables the loop to operate as a magnetic-field radiator, where the current circulates around the loop to generate a magnetic field normal to the loop plane. The loop's placement within the reinforced concrete column allows investigation of electromagnetic coupling between the antenna element and the surrounding carbon steel rebars, providing insights into the feasibility of using structural metals as integrated radiators in smart-building communication systems.

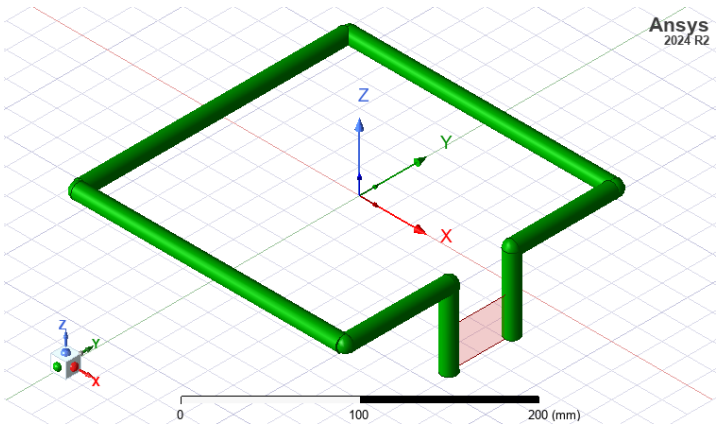

Figure 2. Loop Antenna Configuration

The metallic element selected for the embedded loop antenna is stainless steel with a diameter of approximately 1.2 cm. It is modeled as an embedded conductor within the reinforced concrete structure to emulate realistic building conditions. One of the original stirrups in the four-rebar configuration is replaced by the loop antenna, maintaining structural integrity while enabling electromagnetic analysis. The surrounding concrete and air domains are assigned appropriate dielectric properties to evaluate their effects on the antenna's resonant frequency, impedance characteristics, and radiation performance.

C. Simulation Model

Electromagnetic simulations are conducted using Ansys HFSS, a full-wave three-dimensional finite element method (FEM) solver widely utilized in advanced antenna design and electromagnetic analysis. HFSS is selected due to its capability to accurately model complex geometries, incorporate realistic material properties, and predict the electromagnetic behavior of antennas under structural and environmental constraints. This allows comprehensive evaluation of the antenna's performance, including its resonant characteristics, impedance response, and field distribution within the reinforced concrete environment.

Adaptive meshing is employed, and a frequency sweep from 100 MHz to 1.400 MHz are applied to ensure accurate and reliable simulation results. The wide frequency range enables identification of the antenna's resonant behavior and its impedance variation across the sub-GHz spectrum relevant to IoT and smart-building communication bands.

The simulation model consists of an air box with radiation boundary conditions, a concrete column structure, and a lumped port positioned across a small gap in the loop conductor to excite the antenna,

emulating the feed from an IoT radio. The loop antenna is surrounded by a vacuum region of approximately 1 cm. This configuration ensures that the antenna is not immediately influenced by the concrete medium, thereby enabling precise evaluation of its reflection coefficients and electromagnetic field distributions while considering its integration within structural elements. Figure 3 illustrates the simulation model.

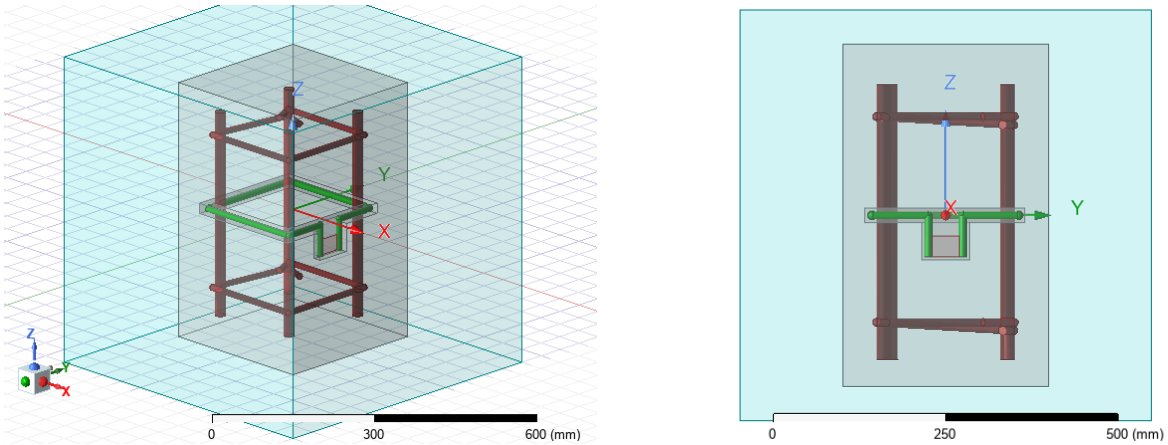

(a) (b)

Figure 3. Building-Embedded Loop Antenna Simulation Model (a) Dimetric Projection (b) Front View Configuration

The key simulation parameters for the embedded metallic structures are presented in Table 1. These parameters define the antenna geometry, material composition, boundary setup, and excitation conditions necessary to ensure accurate modeling within the concrete structure. The selected configuration aims to replicate realistic construction environments and evaluate the electromagnetic performance of the embedded antenna under practical conditions.

Table 1. Simulation Parameters

Parameter	Value
Target Frequency	700 MHz
Frequency Range	100–1.400 MHz
Antenna Type	Quarter-Wavelength Loop
Antenna Material	Stainless Steel
Loop Dimension	Rectangular 21 cm x 21 cm
Feed Gap	5 cm
Feed Section Length	6 cm
Conductor Diameter	1.2 cm
Air Gap Layer	1 cm
Reinforcing Bar	4 Carbon Steel
Stirrup Spacing	15 cm
Embedding Medium	Concrete
Boundary Condition	Radiation (Open)
Excitation	Lumped Port 50 Ω (Base)

III. Results and Discussion

The performance of the building-embedded loop antenna system is analyzed through key electromagnetic parameters relevant to Smart City IoT network applications. The evaluation focuses on: (1) Return loss (S11), which identifies the resonant frequency and assesses impedance matching quality within the concrete medium; (2) Radiation pattern, which illustrates the spatial energy distribution and verifies the

omnidirectional coverage essential for IoT connectivity; and (3) Gain, which represents the power efficiency and determines the antenna's effectiveness for low-power, long-range communication in building-integrated Smart City environments.

A. Return Loss and Resonant Frequency

The measured return loss and resonant frequency characteristics of the building-embedded loop antenna are presented in Figure 4. The measurement results exhibit a distinct resonant peak at the target frequency of 700 MHz, with a return loss value of approximately –20.95 dB, indicating excellent impedance matching between the antenna and the IoT transceiver system. These results are consistent with the analytical predictions derived from the quarter-wavelength approximation, confirming the accuracy of the theoretical design and the reliability of the proposed configuration.

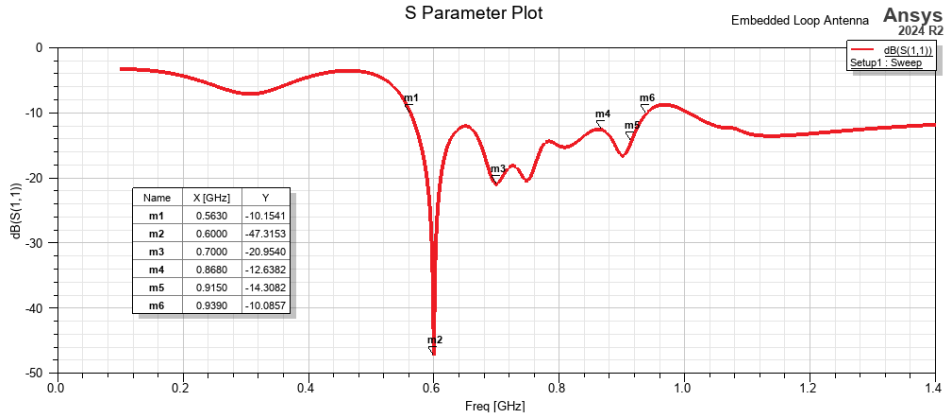

Figure 4. Simulated Return Loss of Embedded Loop Antenna

The low reflection coefficient suggests minimal power loss due to impedance mismatch, ensuring efficient signal transmission. The –10 dB impedance bandwidth of the antenna is approximately 376 MHz, covering the frequency range from 563 MHz to 939 MHz, which is sufficient for reliable IoT communication in smart city applications.

The Voltage Standing Wave Ratio (VSWR), as illustrated in Figure 5, serves as a crucial parameter to assess the impedance matching between the antenna and its associated transmission line or transceiver.

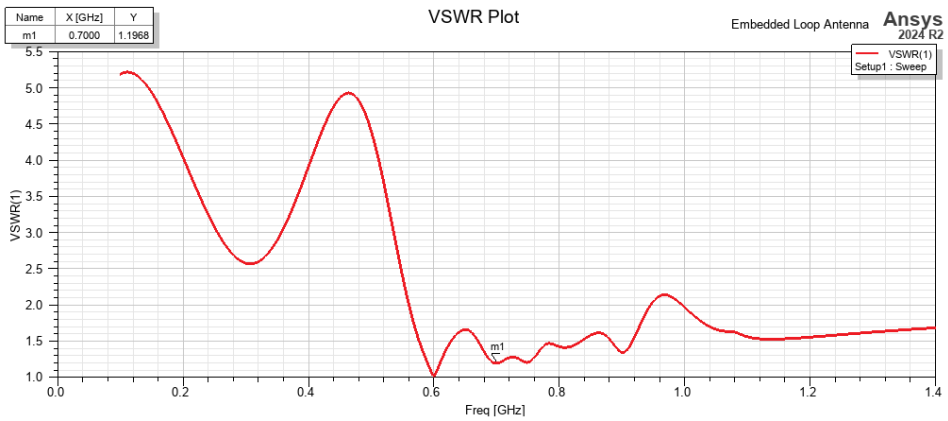

Figure 5. Simulated VSWR of Embedded Loop Antenna

A VSWR value approaching unity signifies an optimal match, where signal reflections are minimized and power transfer efficiency is maximized. In this study, the measured VSWR at the resonant frequency of 700 MHz is 1.196, confirming that the building-embedded loop antenna achieves excellent impedance conformity with the IoT transceiver system. This low VSWR value ensures that the majority of the

transmitted power is effectively radiated, thereby minimizing insertion losses and enhancing the overall reliability and stability of wireless communication in smart city IoT networks.

The observed return loss and wide impedance bandwidth indicate that the proposed building-embedded loop antenna is highly suitable for Low-Power Wide-Area Network (LPWAN) applications, which require long-range connectivity and low power consumption for large-scale IoT deployments. LPWAN technologies such as LoRaWAN, NB-IoT, Z-Wave, and ZigBee operate within sub-GHz and ISM frequency bands, typically between 700 MHz, 868 MHz, and 915 MHz, to achieve extended coverage with minimal energy use. LoRaWAN provides ultra-long-range communication for sensors and smart meters, while NB-IoT offers cellular-grade connectivity optimized for low-throughput IoT devices. Similarly, Z-Wave and ZigBee are widely used for smart home automation and industrial monitoring due to their low latency and reliable mesh networking capabilities. The antenna's excellent impedance matching with a return loss of –20.95 dB and its broad bandwidth of 376 MHz therefore ensure compatibility with these LPWAN protocols, supporting seamless integration into multi-standard smart city IoT ecosystems.

B. Radiation Characteristics

The radiation characteristics play a crucial role in evaluating the overall performance of the building-embedded loop antenna system, as they determine the antenna's ability to effectively transmit and receive signals within smart city IoT networks. In such environments, antennas are expected to provide stable and wide-area coverage despite the presence of complex structural and electromagnetic interferences. Therefore, analyzing the radiation behavior offers valuable insight into how the antenna performs when integrated within building materials.

The radiation characteristics shown in Figure 6 illustrate both the two-dimensional (2D) and three-dimensional (3D) radiation patterns of the proposed antenna at the resonant frequency of 700 MHz. These patterns provide a comprehensive visualization of the antenna's directional distribution and radiated power, serving as the basis for evaluating its performance in embedded configurations.

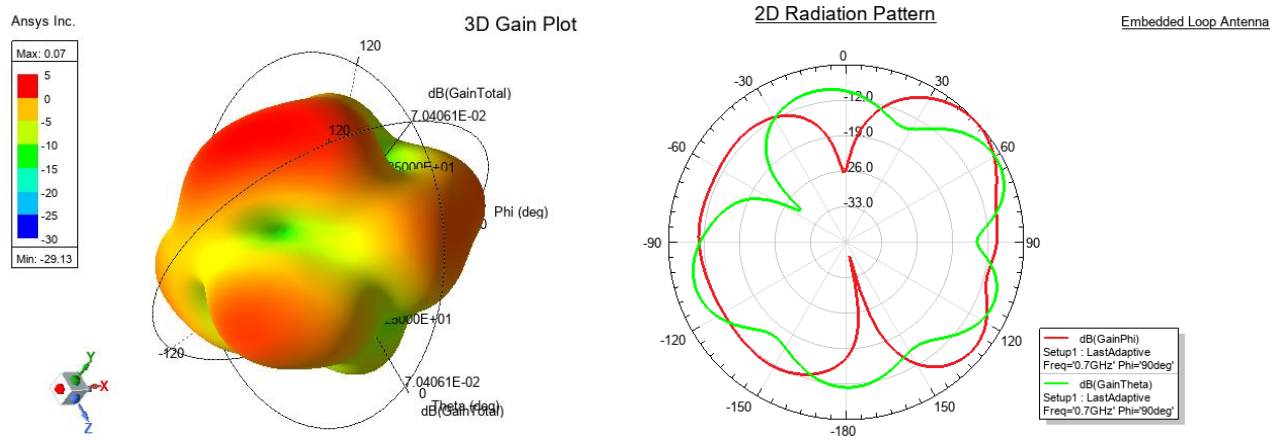

(a) (b)

Figure 6. Radiation Characteristics with Air Gap Layer (a) 3D Gain Plot (b) 2D Radiation Pattern

The simulated total gain of the building-embedded loop antenna with a 1 cm air gap layer is approximately 0.07 dB, while its directivity reaches 6 dB. This condition indicates that although the antenna maintains good directional radiation capability, a significant portion of the radiated power is absorbed or dissipated within the surrounding building materials. The air gap introduces partial impedance mismatch and additional field coupling losses, reducing the effective gain even though the directional property remains stable. The difference between gain and directivity reflects power attenuation caused by dielectric absorption in concrete and electromagnetic coupling with nearby metallic reinforcements.

In contrast, when the antenna is directly embedded without the air gap, as illustrated in Figure 7, the simulated total gain increases to 1.77 dB, while the directivity reaches 7.75 dB, indicating improved

radiation efficiency and stronger power concentration. This comparison confirms that the air gap acts as a lossy transitional region, slightly degrading the overall radiation performance. Nevertheless, even with reduced gain, the antenna maintains a stable radiation pattern and adequate field strength for low-power IoT communication.

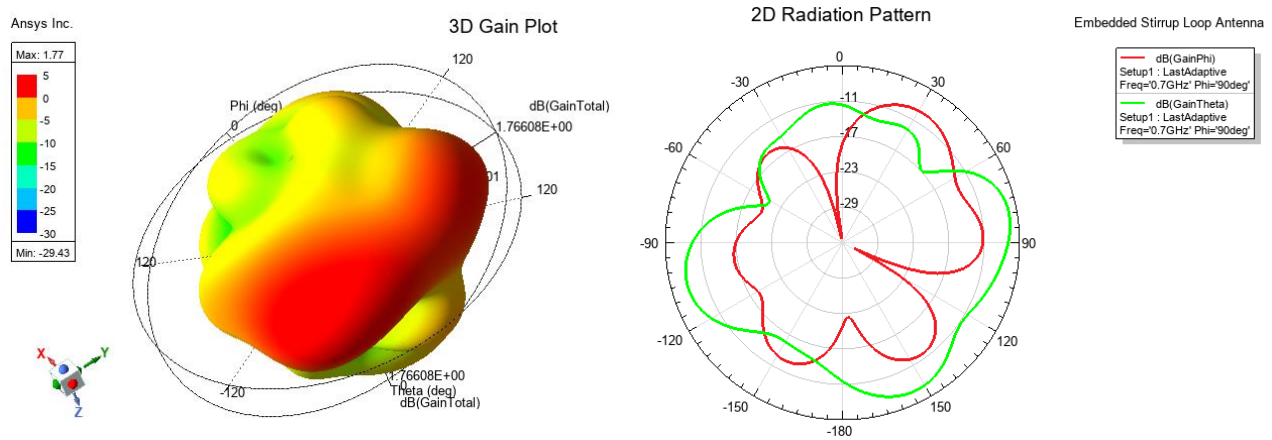

(a) (b)

Figure 7. Radiation Characteristics without Air Gap (a) 3D Gain Plot (b) 2D Radiation Pattern

The radiation pattern of the building-embedded loop antenna, as depicted in both 2D and 3D plots, exhibits a generally omnidirectional shape in the H-plane; however, it is not perfectly circular. Minor distortions and asymmetries are observed, mainly caused by the interaction between the electromagnetic fields and nearby concrete and metallic structures. These irregularities slightly affect the uniformity of field distribution but do not significantly degrade overall coverage performance.

In the E-plane, the radiation pattern demonstrates a figure-eight-like shape with slight asymmetry, attributed to partial field cancellation caused by electromagnetic coupling with surrounding structural materials and boundary constraints of the embedded environment. These distortions deviate from the ideal omnidirectional response, indicating that the presence of concrete and metallic components modifies the surface current distribution along the loop. Nevertheless, the antenna preserves adequately broad radiation coverage suitable for low-power IoT communication, confirming that structural embedding can maintain acceptable radiation performance under practical construction conditions.

In embedded environments, such attenuation is generally expected because the electromagnetic energy interacts with lossy building materials before reaching free space. These results highlight the importance of optimizing the embedding configuration to balance structural integration and radiative efficiency, ensuring mechanical protection, stable electromagnetic performance, and architectural practicality in smart city IoT applications.

C. Practical Considerations and Limitations

In practical applications, embedding loop antennas within building structures offers mechanical protection, architectural integration, and environmental durability. However, surrounding materials introduce electromagnetic challenges such as dielectric absorption, impedance detuning, and coupling losses from nearby metallic reinforcements. Long-term exposure to moisture may also cause corrosion, altering conductivity and degrading performance; thus, corrosion-resistant coatings or composite materials are recommended. Performance optimization can be achieved through controlled air gaps, low-loss dielectric coatings, and placement in regions with lower permittivity. Although the resulting gain and bandwidth may limit long-range communication, the antenna remains suitable for IoT Networks.

This study is limited to simulation-based evaluation under controlled conditions. Future work will involve fabrication and experimental validation in real concrete environments, including measurements of return loss, radiation pattern, and gain, to establish reliable design guidelines for practical building-embedded antenna systems in smart city infrastructures.

IV. Conclusions

In summary, this study aimed to evaluate the performance of building-embedded loop antenna systems for Smart City IoT networks. The simulation results confirmed that the designed antenna successfully achieved the targeted resonant frequency of 700 MHz with a return loss of –20.95 dB and a VSWR of 1.196, indicating excellent impedance matching and minimal reflection. The antenna also provided an impedance bandwidth of approximately 376 MHz (563 MHz to 939 MHz), ensuring compatibility with various IoT communication standards such as LoRaWAN, NB-IoT, Z-Wave, and ZigBee.

Although the total gain was reduced due to dielectric absorption and coupling with surrounding building materials, the radiation pattern remained generally omnidirectional, offering adequate coverage for low-power IoT nodes. The presence of a 1 cm air gap layer decreased the total gain to 0.07 dB compared to 1.77 dB in a fully embedded configuration, highlighting the importance of optimizing the embedding structure for improved efficiency. This observation further confirms that electromagnetic interactions within the building medium significantly influence antenna radiation behavior and must be carefully managed in practical implementations.

Therefore, the results demonstrate that building-embedded loop antennas can serve as functional communication elements in smart building infrastructures while maintaining architectural integrity. Future research will focus on fabrication, experimental validation, and long-term performance evaluation in real concrete environments to establish practical design guidelines for smart city applications.

V. Aknowledgment

The authors gratefully acknowledge the availability of Ansys HFSS under an academic research license provided by Department of Electrical Engineering University of Cokroaminoto Makassar, which was instrumental in conducting the electromagnetic simulations presented in this study.

This research was funded by the Ministry of Higher Education, Science, and Technology of the Republic of Indonesia, through the Directorate General of Research and Development, under the Basic Research Scheme for the 2025 Fiscal Year.

VI. References

[1] J. Rita, J. Salvado, H. d. Rocha, and A. Espírito-Santo, “A comprehensive review of IoT standards: The role of IEEE 1451 in smart cities and smart buildings,” Smart Cities, vol. 8, no. 4, p. 108, 2025.
[2] M. Whaiduzzaman et al., “A review of emerging technologies for IoT-based smart cities,” Sensors, vol. 22, no. 23, p. 9271, 2022.
[3] M. Zaman, N. Puryear, S. Abdelwahed, and N. Zohrabi, “A review of IoT-based smart city development and management,” Smart Cities, vol. 7, no. 3, pp. 1462–1501, 2024.
[4] R. Ahmed Osman and A. I. Zaki, “Energy-efficient and reliable Internet of Things for 5G: A framework for interference control,” Electronics, vol. 9, no. 12, p. 2165, 2020.
[5] K. Majumder, S. Pramanik, and J. Goswami, “Implementation of smart building using Internet of Things (IoT),” in Real-World Applications and Implementations of IoT. Studies in Smart Technologies, A. Acharyya, P. Dey, and S. Biswas, Eds. Singapore: Springer, 2025.
[6] M. Mishra, P. B. Lourenço, and G. V. Ramana, “Structural health monitoring of civil engineering structures by using the internet of things: A review,” Autom. Constr., vol. 132, p. 103936, 2022.
[7] U. Um-e-Habiba, I. Ahmed, M. Asif, H. H. Alhelou, and M. Khalid, “A review on enhancing energy efficiency and adaptability through system integration for smart buildings,” J. Build. Eng., vol. 89, p. 109354, 2024.
[8] M. Albzaie, “Smart materials and smart structures: Transforming engineering and infrastructure,” Int. J. Civil Struct. Eng. Res., vol. 12, no. 2, pp. 42–47, 2024.
[9] M.-Q. Cao, T.-T. Liu, Y.-H. Zhu, J.-C. Shu, and M.-S. Cao, “Developing electromagnetic functional materials for green building,” J. Build. Eng., vol. 45, p. 103496, 2022.
[10] N. Kumar, P. Kumar, and M. Sharma, “Reconfigurable MIMO antenna for IoT wireless applications controlled by embedded system,” J. Telecommun. Inf. Technol., vol. 96, no. 2, pp. 32–40, 2024.
[11] C. A. Balanis, Antenna Theory: Analysis and Design, 4th ed. Wiley, 2016.

[12] S. Khan et al., "Antenna systems for IoT applications: A review," Discover Sustainability, vol. 5, p. 412, 2024.
[13] R. Hussain, S. I. Alhuwaimel, A. M. Algarni, K. Aljaloud, and N. Hussain, "A compact Sub-GHz wide tunable antenna design for IoT applications," Electronics, vol. 11, no. 7, p. 1074, 2022.
[14] L. Inclán-Sánchez, "Performance Evaluation of a Low-Cost Semitransparent 3D-Printed Mesh Patch Antenna for Urban Communication Applications," Electronics, vol. 13, no. 1, art. no. 153, Dec. 2023, doi: 10.3390/electronics13010153.
[15] A. Z. Jusoh, N. F. Husain, N. F. Abdul Malek, F. N. Mohd Isa, and S. Y. Mohamad, "Design of miniaturized antenna for IoT applications using metamaterial," IIUM Eng. J., vol. 24, no. 1, pp. 122–137, 2023.
[16] A. Cozza, "Understanding the apparently poor conductivity of galvanized steel plates," IEEE Access, vol. 9, pp. 149228–149238, 2021.
[17] A. Cosoli, M. Mobili, M. Tittarelli, and L. Cristofolini, "Dielectric properties of hardened cement pastes measured by broadband electromagnetic characterization," Appl. Sci., vol. 10, no. 24, p. 9152, 2020.
[18] G. N. Vizi and G. A. E. Vandenbosch, "Building materials and electromagnetic radiation: The role of material and shape," J. Build. Eng., vol. 5, pp. 96–103, 2016.
[19] X. Chen and Z. Zheng, "A wideband bow-tie slot antenna embedded in dielectric for 5G communication," in Proc. IEEE Int. Conf. Microw. Millim. Wave Technol. (ICMMT), 2023, pp. 1–3.
[20] L. Vähä-Savo, K. Haneda, C. Icheln, and X. Lü, "Electromagnetic-thermal analyses of distributed antennas embedded into a load bearing wall," arXiv preprint, 2022.
[21] L. Vähä-Savo, L. Veggi, E. M. Vitucci, C. Icheln, V. Degli-Esposti, and K. Haneda, "Analytical characterization of a transmission loss of an antenna-embedded wall," IEEE Open J. Antennas Propag., vol. 5, no. 6, pp. 1765–1772, 2024.
[22] J. Tan, Y. Shao, J. Zhang, and J. Zhang, "Empirical formulas for performance prediction of concrete embedded antenna," Univ. Sheffield, 2022.
[23] O. S. Hassan, M. Saif ur Rahman, A. A. Mustapha, S. Gaya, M. A. Abou-Khousa, and W. J. Cantwell, "Inspection of antennas embedded in smart composite structures using microwave NDT methods and X-ray computed tomography," Measurement, vol. 226, p. 114086, 2024.
[24] S. Shailesh, G. Srivastava, and S. Kumar, "A flexible reconfigurable MIMO antenna for IoT-enabled smart systems," Int. J. Antennas Propag., vol. 2024, p. 7557178, 2024.
[25] A. Bal, J. W. Baur, D. J. Hartl, G. J. Frank, T. Gibson, H. Pan, and G. H. Huff, "Multi-layer and conformally integrated structurally embedded vascular antenna (SEVA) arrays," Sensors, vol. 21, no. 5, p. 1764, 2021.
[26] C. Milarokostas, D. Tsolkas, N. Passas, and L. Merakos, "A comprehensive study on LPWANs with a focus on the potential of LoRa/LoRaWAN systems," IEEE Commun. Surveys Tuts., vol. 25, no. 1, pp. 825–867, 2022.
[27] A. Mahmood, L. Beltramelli, S. F. Abedin, M. Gidlund, and K. Yang, "Industrial IoT in 5G-and-beyond networks: Vision, architecture, and design trends," IEEE Trans. Ind. Informat., vol. 18, no. 6, pp. 4122–4137, 2022.
[28] F. Tubbal, L. Matekovits, dan R. Raad, "Antenna Designs for 5G/IoT and Space Applications, 2nd Edition," Electronics, vol. 14, no. 7, art. no. 1308, Mar. 2025, doi: 10.3390/electronics14071308.
[29] A. Salmi, M. Capek, L. Jelinek, A. Lehtovuori, dan V. Viikari, "Optimization of Embedded Element Patterns of Reactively Loaded Antenna Arrays," IEEE Transactions on Antennas and Propagation, Apr. 2025.
[30] N. Zain, A. H. . Udin, and M. I. . M, "Smart Antenna Based IEEE 802.11 MAC Protocol for Radar Networks", Computer, Control System, and Networking Journal, vol. 4, no. 3, pp. 220-231, Jul. 2025.